Cell Proliferation

Cell Prolif., 2012, **45**, 545–556 doi: 10.1111/j.1365-2184.2012.00847.x

The mechanisms of nadroparin-mediated inhibition of proliferation of two human lung cancer cell lines

Y. Carmazzi*, M. Iorio†, C. Armani‡, S. Cianchetti*, F. Raggi§, T. Neri*, C. Cordazzo*,$, S. Petrini*, R. Vanacore†, F. Bogazzi§, P. Paggiaro* and A. Celi*

**Laboratory of Respiratory Cell Biology, Cardiac, Thoracic and Vascular Department, University of Pisa and University Hospital of Pisa, Pisa, Italy, †Immunohematology Unit II, University of Pisa and University Hospital of Pisa, Pisa, Italy, ‡Cardiovascular Research Laboratory, Cardiac, Thoracic and Vascular Department, University of Pisa and University Hospital of Pisa, Pisa, Italy, §Endocrinology and Metabolism Department, University of Pisa and University Hospital of Pisa, Pisa, Italy and $National Institute for Cardiovascular Research (INRC), Bologna, Italy*

Received 6 February 2012; revision accepted 5 July 2012

Abstract

Objectives: Clinical data suggest that heparin treatment improves survival of lung cancer patients, but the mechanisms involved are not fully understood. We investigated whether low molecular weight heparin nadroparin, directly affects lung cancer cell population growth in conventionally cultured cell lines.

Materials and methods: A549 and CALU1 cells' viability was assessed by MTT and trypan blue exclusion assays. Cell proliferation was assessed using 5-bromo-2-deoxyuridine incorporation. Apoptosis and cell-cycle distribution were analysed by flow cytometry; cyclin B1, Cdk1, p-Cdk1 Cdc25C, p-Cdc25C and p21 expressions were analysed by western blotting. mRNA levels were analysed by real time RT-PCR.

Results: Nadroparin inhibited cell proliferation by 30% in both cell lines; it affected the cell cycle in A549, but not in CALU-1 cells, inducing arrest in the G_2/M phase. Nadroparin in A549 culture inhibited cyclin B1, Cdk1, Cdc25C and p-Cdc25C, while levels of p-Cdk1 were elevated; p21 expression was not altered. Dalteparin caused a similar reduction in A549 cell population growth; however, it did not alter cyclin B1 expression as expected, based on previous reports. Fondaparinux caused minimal inhibition of A549 cell population growth and no effect on either cell cycle or cyclin B1 expression.

Conclusions: Nadroparin inhibited proliferation of A549 cells by inducing G_2/M phase cell-cycle arrest that was dependent on the Cdc25C pathway, whereas CALU-1 cell proliferation was halted by as yet not elucidated modes.

Correspondence: A. Celi, Cardiac, Thoracic and Vascular Department, Cisanello Hospital, via Paradisa, 2, 56124 Pisa, Italy. Tel: (+)39 050996942; Fax: (+)39 050996947; E-mail: alessandro.celi@med.unipi.it

Introduction

Lung cancer is the leading cause of cancer-related death in industrialized countries (1) and despite enormous efforts to optimize available therapeutic options, overall 5-year survival rate for this disease is still approximately only 15% (2). Thus, research in the field of lung cancer biology is very active in an attempt to develop novel therapeutic strategies (3).

As cancer patients are at increased risk of developing thromboembolic disorders, heparin and heparin derivatives have long been used as therapeutic agents to these ends, in these patients. Clinical studies have suggested that low molecular weight heparins (LMWHs) improve life expectancy of cancer patients, including those with lung cancer (4–6). However, the basis for such benefit, which goes beyond mere reduction of fatal thromboembolic events, is not fully understood. Several possible explanations have been proposed. Cancers represent 'Darwinian systems' and cancer cells have highly accelerated mutation rates, which allow them to select characteristics that are favourable for their proliferation and survival (7). Thus, it is likely that the hypercoagulable state induced by cancer, whatever its mechanisms, is beneficial to survival of the neoplasm. It can be speculated that anticoagulants might exert anti-cancer consequences simply by depriving tumours of the beneficial effect of activation of the coagulation cascade that they actively promote. Heparins have also been shown to inhibit P-selectin-mediated cell–cell adhesion

mechanisms. Thus, these molecules might prevent interaction of cancer cells with activated platelets, an essential step in the so-called metastatic cascade (8). As tumours are angiogenesis-dependent, the long known anti-angiogenic effects of certain LMWHs on VEGF-mediated angiogenesis *in vivo* might contribute to reported beneficial outcomes of LMWHs for cancer patients (9). Finally, the possibility that LMWHs directly interfere with cancer cell population growth has been investigated. Vascular smooth muscle cell proliferation is inhibited by unfractionated heparin (UFH) (10) through disregulation of the cell cycle (11). Evidence has also been gathered that suggests an effect of some LMWHs on cancer cell population growth, although data available have been largely conflicting [see (12) for a review]. Several groups have investigated some of the mechanisms by which different LMWHs potentially modulate cell proliferation. Dalteparin has been shown to inhibit the extracellular signal-regulated kinase (ERK) pathway (12). Chen *et al.* have demonstrated that dalteparin interferes with lung cancer cell population growth through inhibition of p21 and p27 proteins, thus causing arrest in the G_0/G_1 phase of the cell cycle (13).

LMWHs are prepared by enzymatic or chemical depolymerization of UFH. As the methods of fractionation are different, each LMWH has a unique chemical, biochemical, biophysical, and biological profile, which results in different biological actions, as well as in different clinical activities (14,15).

The aim of this study was to investigate whether the low molecular weight heparin, nadroparin, interferes with lung cancer cell population growth, and the mechanisms involved.

Materials and methods

Cell lines, cell culture and reagents

Human lung adenocarcinoma A549 cell line and human epidermoid carcinoma CALU-1 cell line were obtained from the Cell Bank of Interlab Cell Line Collection (ICLC, Genova, Italy). Although established decades ago, both cell lines are still extensively used as models of human lung cancer biology. A549 cells were cultured in Dulbecco's modified Eagle's medium (DMEM) supplemented with 10% heat-inactivated foetal bovine serum (FBS), L-glutamine (2 mmol/l), penicillin (100 U/ml) and streptomycin (100 μg/ml); CALU-1 cells were cultured in McCoy's 5A medium supplemented with 10% heat-inactivated FBS, L-glutamine (2 mmol/l), penicillin (100 U/ml) and streptomycin (100 μg/ml). Cell lines were maintained in a humidified atmosphere of 95% air and 5% CO_2 at 37 °C, and subcultured when 60–80% confluence was reached. DMEM, McCoy's 5A and other standard reagents for cell culture were purchased from Sigma-Aldrich (Milan, Italy).

Chemicals and immunoreagents

Trypan blue, (3-(4,5-dimethylthiazol-2-yl)-2,5-diphenyltetrazolium bromide (MTT), dimethyl sulphoxide, Dulbecco's phosphate-buffered saline (PBS), 0.25% trypsin-EDTA solution, colchicine and protease inhibitors [aprotinin, pepstatin A, leupeptin, phenyl methyl sulphonyl fluoride (PMSF)] were obtained from Sigma-Aldrich.

Nadroparin (Fraxiparina®; Glaxo Smith Kline, London, UK), Dalteparin (Fragmin®; Pharmacia, Stockholm, Sweden) and Fondaparinux (Arixtra®; Glaxo Smith Kline) were obtained as standard drug formulations. Cisplatin was kindly obtained from University Hospital of Pisa. Drugs were diluted to required concentrations with culture medium immediately before each test.

Mouse monoclonal antibodies against cyclin B1, Cdk1, Cdc25C and p21, goat anti-mouse horseradish peroxidase labelled secondary antibody, anti-human β-actin and anti-human α-tubulin mouse monoclonal antibodies were purchased from Santa Cruz Biotechnology (Santa Cruz, CA, USA); rabbit monoclonal antibodies against p-Cdk1 (Tyr15) and p-Cdc25C (Ser216), anti-human β-actin rabbit monoclonal and goat anti-rabbit horseradish peroxidase labelled secondary antibody were purchased from Histo-Line Laboratories (Epitomics, Milan, Italy).

Low molecular weight heparins

LMWHs are prepared either by fractionation of UFH, usually derived from porcine intestinal mucosa, or by its depolymerization (16). Each of these LMWHs has a characteristic molecular weight profile and biological activity, in terms of anti-FXa and anti-FIIa potency. All molecules share the characteristic that 60% of the species are below 8000 Da (range 4000–7000 Da) with chain length of 12–22 polysaccharides and anti-FXa: anti-FIIa ratio ranging from 1.5 to 3.5 (16).

Several methods of partial depolymerization are used, of which the most common is deaminative cleavage with nitrous acid or organic nitrite. This method breaks heparin chains at N-sulphated glucosamine residues, leaving characteristic anhydromannose reducing-end residue, which is usually reduced to anhydromannitol. An alternative approach is characterized by chemical or enzymatic depolymerization, which leaves unsaturated uronic acid residue at the non-reducing terminus; finally, oxidative depolymerization represents the third method

in use; this method does not leave a specific 'signature' structure of the product.

At the end of each method, a mixture of heparin fragments with different numbers of oligosaccharides and higher and/or lower sulphur/carbon ratio than whole heparin, is obtained. The heterogeneity of LMWHs depends not only on different depolymerization processes but also on animal and organ source, and on extraction and purification procedures.

These agents may also be characterized by presence of specific chemical end groups; for example, enoxaparin, which is prepared by benzylation followed by alkaline hydrolysis of UFH, exhibits a double bond at the non-reducing end and presence of a unique bicyclic structure, namely 1,6 anhydromanno glucose or mannose, or both, at the reducing end. Similarly, other LMWHs, such as dalteparin, nadroparin, tinzaparin, and parnaparin, exhibit specific structural and molecular characteristics that may contribute to their own unique biochemical and pharmacological profiles (17). As a consequence, LMWHs compose a group of similar yet different, drug agents and their properties vary significantly in terms of molecular weight profiles, characteristic end residues, oligosaccharide composition and SO_3^-/COO^- ratios.

Cell population growth assays

To assess cell population growth and viability, cell counting was performed after both MTT and trypan blue dye exclusion assays. For MTT assays, 5×10^3 cells/well were seeded into 96-well plates and were incubated overnight. Cells were then washed twice in PBS 1X, and to synchronize them in quiescence, they were cultured in serum-free DMEM for 24 h. Cells were then changed to 0.1% FBS-DMEM with or without the test drug (40 IU/ml, unless otherwise specified) for 2 h. After 2 h, they were serum-stimulated with DMEM containing 10% serum, with or without test drug for 24 h. MTT (100 μl at 5 mg/ml) was added to each well and cells were incubated at 37 °C for further 2 h. Formazan crystals formed by MTT metabolism were solubilized by addition of 100 μl of dimethyl sulphoxide to each well and absorbance (A) was measured at a wavelength of 570 nm with background subtraction at 630-690 nm using a microplate reader (Titertek Multiskan MCC ELISA reader; Flow Laboratories, McLean, VA, USA). Cell population growth was expressed as a percentage of control values. Rate of inhibition was calculated using the following equation:

$$\text{Rate of population growth inhibition}(\%) = (1 - A_{\text{treated}}/A_{\text{control}}) \times 100.$$

For trypan blue dye exclusion assays, 5×10^4 cells/well were plated in 24-well plates, and then treated exactly as described above for the MTT assay. At the end of 24 h treatment, cells were detached by gentle trypsinization, pelleted and resuspended in DMEM containing 0.04% (w/v) trypan blue solution, and counted using a Nebauer Chamber under an inverted microscope. Viable cells exclude the dye, while non-viable cells absorb it and thus appear blue.

Cell proliferation assay by bromodeoxyuridine incorporation

Cell proliferation was measured using a commercially available kit (Cell Proliferation ELISA, BrdU colorimetric kit; Roche Applied Science, Penzberg, Germany). Briefly, cells were seeded in 96-well plates at 5×10^3/well and treated exactly as described above. At the end of the treatment period, cells were incubated in 20 μl bromodeoxyuridine (BrdU)-labelling solution (final concentration, 10 μM) per well for 4 h, dried, fixed and detected using an anti-BrdU antibody according to the manufacturer's instructions. Finally, absorbance was measured using a microplate reader at 450 nm with reference wavelength of 690 nm.

Assessment of apoptosis

Apoptosis was measured using a commercially available kit (Annexin V-FITC Detection Kit; Abcam, Cambridge, UK) according to manufacturer's instructions. In brief, 2×10^5 cells/well were applied to six-well plates and treated exactly as described above; cisplatin (32 μM) treatment was used as positive control. After drug treatment, 5×10^5 cells were resuspended in 500 μl of binding buffer containing 5 μl fluorescein isothiocyanate (FITC) conjugated annexin-V and 5 μl propidium iodide, and incubated in the dark at room temperature for 10 min. Cells were then analysed in a FACScalibur flow cytometer (Beckton Dickinson, San Jose, CA, USA) to differentiate apoptotic cells (annexin-V positive and PI negative, lower right quadrant) from necrotic cells (annexin-V/PI positive, upper right quadrant). Ten thousand events were recorded for each treatment group.

Cell cycle analysis

Cell cycle distribution was analysed by flow cytometry using PI staining. Briefly, 6×10^5 cells were cultured in 10-cm culture dishes, and treated exactly as described above. At the end of the treatment period, 5×10^5 cells were resuspended in 500 μl of binding buffer, DNA

was labelled with PI (50 μg/ml) and incubated at 4 °C for 10 min. Fluorescence was measured using a FACScalibur flow cytometer (Beckton Dickinson). Effects on the cell cycle were determined by changes in percentage of cell distribution at each phase of the cell cycle, and assessed by histograms using CellQuest and the ModFit software (Beckton Dickinson).

Western blot analysis for detection of cyclin B1, Cdk1, p-Cdk1, Cdc25C, p-Cdc25C and p21

Cells (6×10^5) were seeded in 10-cm culture dishes and treated as described above. At the end of the treatment period, cells were washed twice in ice-cold PBS, collected by gentle trypsinization, pelleted and lysed with 200 μl of a solution containing 20 mM Tris–HCl (pH 7.5), 10% glycerol, 137 mM NaCl, 10% sodium dodecyl sulphate (SDS), 1% Triton X-100, 10 mM EDTA and protease inhibitors (aprotinin 1 μg/ml, pepstatin A 1 μg/ml, leupeptin 1 μg/ml and PMSF 1 mM). Cell lysate was cleared by centrifugation at 14 000 *g* for 30 min at 4 °C. Protein content in the supernatant fraction was determined by a commercially available kit based on the Bradford method (Bio-Rad, Hercules, CA, USA), according to the manufacturer's directions. Equal amounts of sample lysate (20–30 μg) were subjected to 10% SDS–polyacrylamide gel electrophoresis, according to Laemmli (18) and proteins were transferred to pure nitrocellulose membranes (Bio-Rad Laboratories). Membranes were blocked with 5% non-fat dry milk (Bio-Rad Laboratories) in TBS-T containing 0.5% Tween 20, 50 mM Tris-HCl (pH 7.6) and 150 mM NaCl for 24 h at 4 °C, then were incubated with mouse anti-cyclin B1 (1:400), anti-Cdk1 (1:400), rabbit anti-p-Cdk1 (1:1000), anti-Cdc25C (1:100), rabbit anti-p-Cdc25C (1:1000) and anti-p21 antibodies (1:100) overnight at 4 °C. Membranes were then incubated in antibody against actin (1:500 dilution), β-actin (1:500 dilution) or α-tubulin (1:3000), and rabbit antibody against β-actin (1:3000), for 1 h at 37 °C, to ensure equal protein loading. At the end of this period, membranes were incubated in horseradish peroxidase conjugated goat anti-mouse antibody (1:1000) and horseradish peroxidase conjugated goat anti-rabbit antibody (1:3000) for 2 h at 37 °C. Finally, membranes were washed twice in TBS-T and once in TBS. Immunoreactive bands were visualized using ECL western blotting detection reagent (Immobilon Western, Chemiluminescence HRP Substrate by Millipore Corporation, Billerica, MA, USA), according to the manufacturer's instructions.

Band intensity was calculated using image analysis software (IMAGEJ version 1.42q; NIH, Bethesda, MD, USA).

Total RNA extraction and cDNA synthesis

Total RNA was extracted from treated samples using a commercially available kit (PerfectPure™ RNA Purification System 5PRIME; Eppendorf, Milan, Italy), according to manufacturer's instructions, and genomic DNA was eliminated using RNase-free DNase I. Purity of total RNA extracted was determined at 260 and 280 nm using a spectrophotometer. RNA samples with absorbance ratio at $OD_{260/280}$ between 1.9 and 2.2 were considered suitable for experimentation.

RNA integrity was verified by 1.5% agarose gel electrophoresis and ethidium bromide staining. First-strand cDNA was synthesized from 1000 ng total RNA subjected to reverse transcription in 20 μl volume, using iScript™ cDNA Synthesis Kit (Bio-Rad Laboratories) according to manufacturer's instructions.

Real time RT-PCR

Gene-specific primer pairs were designed by Bio-Rad using Beacon Designer 7.0, mFold, and synthesized by Invitrogen (Carlsbad, CA, USA). Primers were as follows: cyclin B1, sense 5′-*CTGAAGGTGATGGAGGTAT*-3′ antisense 5′-*GGATTCGGTGGTAGACTT*-3′; Cdk1, sense 5′-*AATCATCTCAGTCCTTATG*-3′ antisense 5′-*AG CCAGGTTGTATAGTTA*-3′; Cdc25C, sense 5′-*GCCA GAGAACTTGAACAG*-3′ antisense 5′-*AATCTTCCTCCA GCATCT*-3′; RPL11, sense 5′-*ACTTCGCATCCGCAAAC TCT*-3′ antisense 5′-*TGTGAGCTGCTCCAACACCTT*-3′; RPL13, sense 5′-*CCTGGAGGAGAAGAGGAAAGAGA*-3′ antisense 5′-*TTGAGGACCTCTGGTGTATTTGTCAA*-3′; HPRT, sense 5′-*AGACTTTGCTTTCCTTGGTCAGG*-3′ antisense 5′-*GTCTGGCTTATATCCAACACTTCG*-3′. All PCR investigations were performed with SYBR Green I chemistry in a MiniOpticon Real-Time PCR System (Bio-Rad). For PCR events, final reaction mixture contained 1 μl of cDNA, 300 nmol/l of each primer, 7.5 μl of iQ SYBR green Supermix (Bio-Rad), and RNase-free water, to complete the reaction mixture volume up to 15 μl. All reactions were run in duplicate. PCR was performed with 'hot-start' denaturation step at 95 °C for 3 min, then carried out for 41 cycles at 95 °C for 5 s and 58 °C for 20 s.

SYBR green fluorescence was read throughout the reaction, allowing continuous monitoring of amount of PCR product amplified. Specificity of amplification was confirmed by melting-curve analysis from subsequent temperature ramp from 60 to 95 °C. Amplification efficiencies were close to 100% for all primer pairs. Comparative Ct (threshold cycle) method has been normalized to 60S ribosomal protein L11 (RPL11), 60S ribosomal protein L13 (RPL13) and hypoxanthine phos-

phoribosyltransferase (HPRT); three stable RNAs in experimental conditions were used to analyse relative changes in gene expression (amount of target = $2^{-\Delta\Delta Ct}$). Data were reported as means ± SD from three independent experiments.

Statistical analysis

Data are expressed as mean ± SEM of n independent experiments. Comparisons of three or more groups were performed by ANOVA, followed by Bonferroni's test. Comparisons between two groups were performed by Student's *t*-test and *P*-value <0.05 was considered statistically significant. All analyses were performed by Prism (GraphPad Software, San Diego, CA, USA).

Results

Figure 1a indicates kinetics of inhibition of A549 lung cancer cell population growth by nadroparin, at different concentrations. At 40 IU/ml, the effect was near-maximal, at 48 h. Figure 1b reveals dose-dependent reduction in number of viable A549 cells at 48 h, as assessed by MTT assay; this reached statistical significance at 20 IU/ml; at 40 IU/ml, nadroparin caused approximately 30% inhibition of number of viable cells. To confirm results obtained from MTT assay, A549 cell population growth was assessed by trypan blue assay. As shown in Fig. 1c, nadroparin (40 IU/ml) caused significant (22%) reduction in number of viable cells. As both MTT and trypan blue exclusion assays are viability tests rather than cell proliferation assays, we used BrdU incorporation to assess the effect of nadroparin on A549 cell proliferation. As shown in Fig. 1d, nadroparin (40 IU/ml) also caused significant (30%) inhibition of cell proliferation.

We then examined whether induction of apoptosis was responsible for anti-proliferative effects of nadroparin. As shown in Fig. 2, percentage of cells positive for annexin V staining and negative for PI staining (that is, apoptotic cells) was not affected by nadroparin treatment (0.86% versus 0.92%). In contrast, cisplatin, a known inducer of apoptosis in cancer cells, including lung cancer cells (19,20) used as a positive control, caused 12% of A549 cells to become apoptotic. Necrosis was not affected by either treatment.

To determine whether mechanisms of cell population growth inhibition by nadroparin were related to cell cycle control, we analysed the cell cycle in A549 cells. Analysis of cell cycle phases was performed by flow cytometry after nadroparin treatment. Figure 3 shows that nadroparin at 40 IU/ml for 48 h induced significant reduction in percentage of A549 cells in G_0/G_1 phase

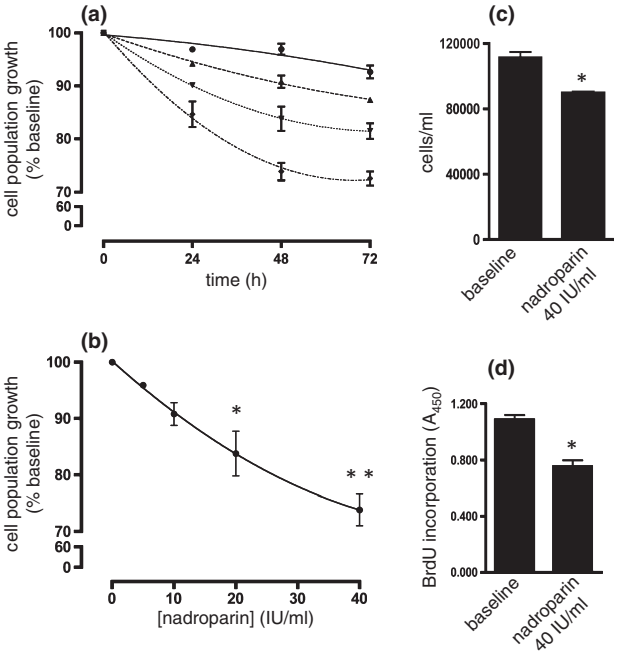

Figure 1. Kinetics (a) and dose–response analysis (b) of effects of nadroparin treatment of A549 cell population growth in MTT reduction assay, and effect of nadroparin on A549 cell population growth determined by trypan blue dye exclusion assay (c) and on A549 cell proliferation determined by BrdU incorporation (d). (a) Cells treated with nadroparin at 5 (●), 10 (▲), 20 (▼) and 40 (♦) IU/ml for 24, 48 and 72 h; (b) Cells treated with nadroparin at different concentrations for 48 h. Data expressed as mean ± SEM of three independent experiments, each performed in quadruplicate. *$P < 0.05$ and **$P < 0.01$ for 20 and 40 IU/ml, respectively, versus untreated cells (ANOVA). (c and d) Cells treated with nadroparin at 40 IU/ml for 48 h. Data are representative of three independent experiments, each performed in quadruplicate. *$P < 0.05$ for 40 IU/ml nadroparin-treated versus -untreated cells (Student's *t*-test).

(45.5 ± 3.2% versus 60 ± 1.6%; $P < 0.05$) and significant increase in percentage of cells in G_2/M phase (21.8 ± 2.3% versus 15.6 ± 1.8%; $P < 0.05$).

The role of cyclin-dependent kinases (Cdks), of Cdk inhibitors (Cdkis) and of Cdk regulatory proteins, cyclins, in regulation of the cell cycle is well established. Specifically, cyclin B1 is regulatory subunit for Cdk1, also known as cdc-2/p34, involved in transition from G_2 phase to mitosis (21). We therefore speculated that nadroparin might affect cyclin B1 expression. Indeed, cyclin B1 antigen expression, as assessed by western blotting, was reduced by nadroparin (Fig. 4a). We also analysed expression of related cell cycle regulatory genes. Real-time RT-PCR analysis demonstrated that cyclin B1 transcript expression was significantly reduced after 48 h nadroparin exposure (Fig. 4b). As inhibition of Cdk1 activity results in G_2/M arrest in various cell lines (22), we also speculated that nadroparin might alter

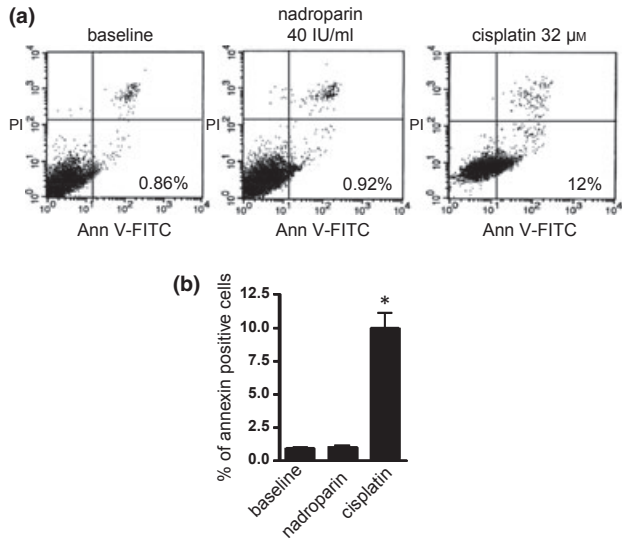

Figure 2. Effect of nadroparin treatment on A549 apoptosis induction, as assessed by flow cytometric analysis. (a) Scatterplots from one representative experiment; (b) Mean ± SEM from three independent experiments $*P < 0.05$ cisplatin versus untreated cells (ANOVA).

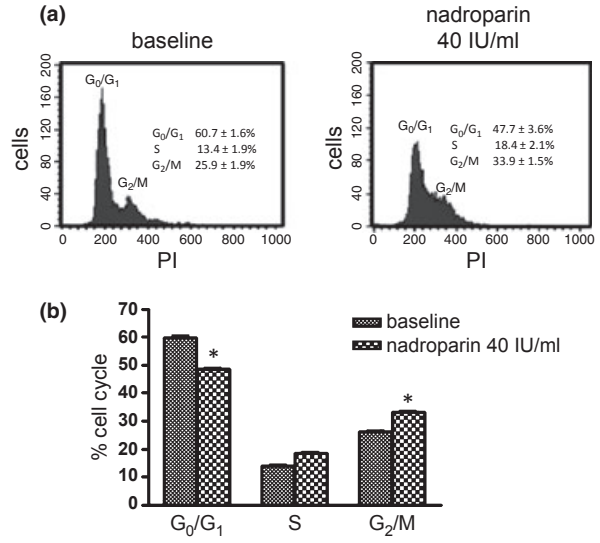

Figure 3. Effect of 48 h nadroparin treatment on A549 cell cycle distribution as assessed by flow cytometric analysis. (a) Histograms from one representative experiment; (b) Mean ± SEM from three independent experiments. $*P < 0.05$ for nadroparin-treated versus -untreated cells for both G_0/G_1 and G_2/M phases (Student's *t*-test).

its expression as well. As shown in Fig. 5a,c, expression levels of protein and mRNA of Cdk1, as assessed by western blotting and real time RT-PCR, were also significantly decreased after nadroparin treatment. In contrast, the expression level of phosphorylated Cdk1 protein (p-Cdk1 Tyr15), as assessed by western blotting, was increased by nadroparin treatment (Fig. 5b).

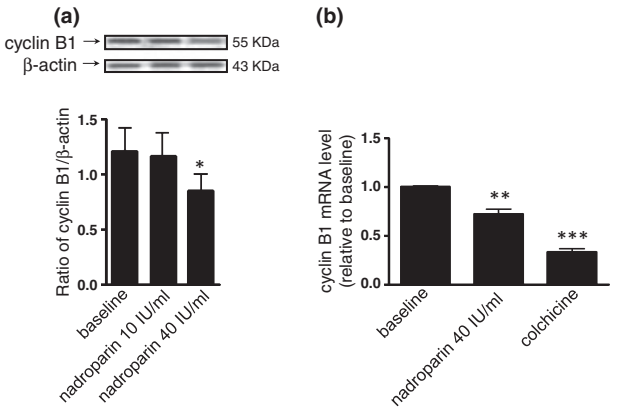

Figure 4. Western blot analysis of the effect of nadroparin on cyclin B1 (a) protein levels and analysis of cyclin B1 (b) mRNA expression in A549 cells. (a) Effect of nadroparin on cyclin B1 protein levels. Blot is representative of three independent experiments. For densitometric analysis of resulting bands, these were quantified using IMAGEJ; data are mean ± SEM from all three experiments. $*P < 0.05$ for nadroparin (40 IU/ml)-treated versus -untreated cells (ANOVA); (b) Effect of nadroparin on cyclin B1 mRNA expression. Data are mean ± SEM from three independent experiments. $**P < 0.01$ for nadroparin (40 IU/ml)-treated versus -untreated cells (ANOVA); $***P < 0.0001$ for colchicine-treated versus -untreated cells (ANOVA).

Cdks are maintained in an inactive state by reversible phosphorylation of Thr 14 and Tyr 15. Activation of Cdks is mediated by dephosphorylation of these residues, in turn caused by Cdc25 family (A, B, and C) of phosphatases (23). To check if Cdk inactivation could be associated with reduced expression or activation of specific phosphatases, we investigated whether nadroparin affects Cdc25C expression and phosphorylation. Indeed, expression of Cdc25C protein and mRNA levels, as assessed by western blotting and real time RT-PCR, were significantly reduced by nadroparin treatment (Fig. 5d,f). Furthermore, expression level of phosphorylated Cdc25C protein (p-Cdc25C Ser216), active form of the phosphatase, as assessed by western blotting, was reduced by nadroparin treatment (Fig. 5e). These results suggest that nadroparin influences transcriptional and post-transcriptional mechanisms of cyclin B1, Cdk1 and Cdc25C.

In addition to Cdks and cyclins, Cdkis are involved in cell cycle control. p21 is a Cdki that tightly regulates activities of cyclin/Cdk enzyme complexes, including cyclin B1/Cdk1 complex. Figure 6 shows that nadroparin treatment did not modulate p21 expression, as assessed by western blotting. In contrast, colchicine [a known inhibitor of tubulin polymerization in cells, including non-small cell lung cancer cells (24)] used as a positive control, caused upregulation of p21 levels, as expected. This result demonstrates that G_2/M phase

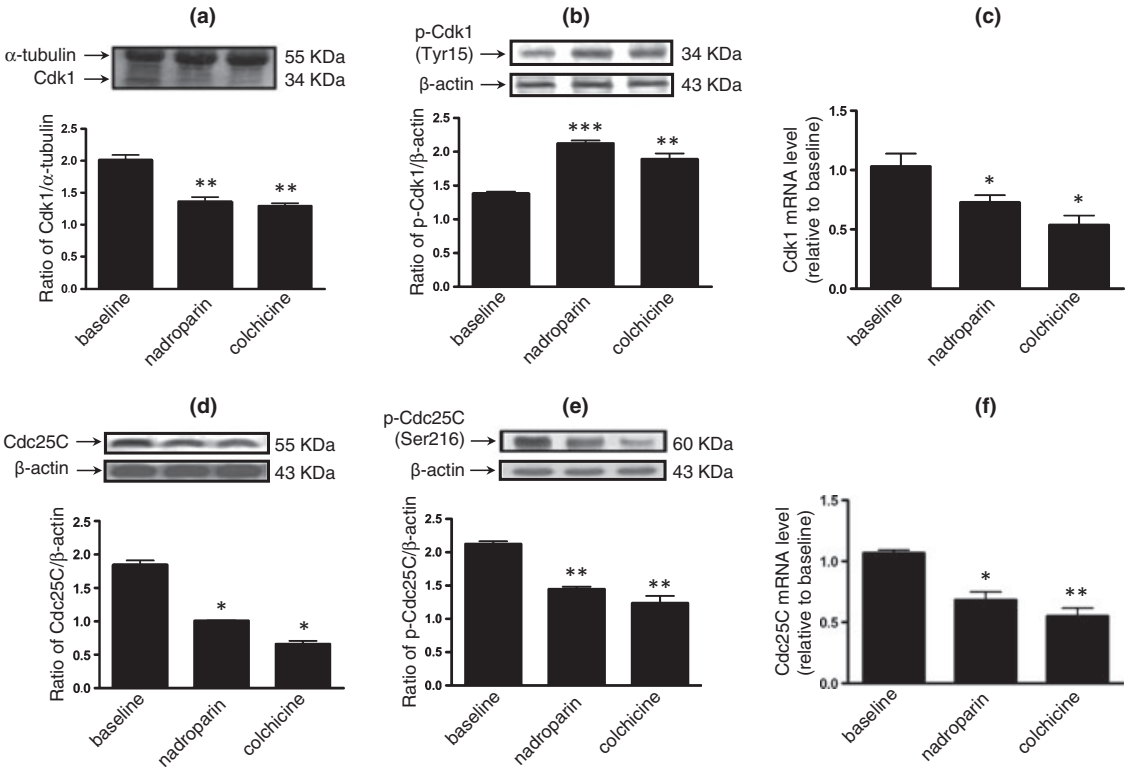

Figure 5. Western blot analysis of the effect of nadroparin on Cdk1 (a), p-Cdk1 (b), Cdc25C (d) and p-Cdc25C (e) protein levels and analysis of Cdk1 (c) and Cdc25C (f) mRNA expression in A549 cells. (a) Effect of nadroparin on Cdk1 protein levels. Blot is representative of three independent experiments. For densitometric analysis, resulting bands were quantified using IMAGEJ; data are mean ± SEM from all three experiments. $^{**}P < 0.01$ for nadroparin (40 IU/ml) and colchicine-treated versus -untreated cells (ANOVA); (b) Effect of nadroparin on p-Cdk1 protein levels. The blot is representative of three independent experiments. For densitometric analysis, resulting bands were quantified using IMAGEJ; data are mean ± SEM from all three experiments. $^{***}P < 0.0001$ for nadroparin (40 IU/ml)-treated versus -untreated cells (ANOVA); $^{**}P < 0.01$ for colchicine-treated versus -untreated cells (ANOVA); (c) Effect of nadroparin on Cdk1 mRNA expression. Data are mean ± SEM from three independent experiments. $^{*}P < 0.05$ for nadroparin (40 IU/ml) and colchicine-treated versus -untreated cells (ANOVA); (d) Effect of nadroparin on Cdc25C protein levels. Blot is representative of three independent experiments. For densitometric analysis, resulting bands were quantified using IMAGEJ; data are mean ± SEM from all three experiments. $^{*}P < 0.05$ for nadroparin (40 IU/ml) and colchicine-treated versus -untreated cells (ANOVA); (e) Effect of nadroparin on p-Cdc25C protein levels. Blot is representative of three independent experiments. For densitometric analysis, resulting bands were quantified using IMAGEJ; data are mean ± SEM from all three experiments. $^{**}P < 0.01$ for nadroparin (40 IU/ml) and colchicine-treated versus -untreated cells (ANOVA); (f) Effect of nadroparin on Cdc25C mRNA expression. Data are mean ± SEM from three independent experiments. $^{*}P < 0.05$ for nadroparin (40 IU/ml)-treated versus -untreated cells (ANOVA); $^{**}P < 0.01$ for colchicine-treated versus -untreated cells (ANOVA).

arrest by nadroparin in A549 cells is not dependent on the p21 pathway.

As previous reports have suggested that LMWH, dalteparin, does not affect cyclin B1 expression by A549 cells (13), we tested the two different molecules in parallel, confirming that they have different effects on cyclin B1 expression (Fig. 7), even though cell population growth was inhibited to a similar extent (not shown).

We then investigated whether nadroparin exerted the same effects on a further lung cancer cell line, CALU-1. Nadroparin caused reduction in CALU-1 cell population growth almost identical to that of A549 cells (data not shown). However, to our surprise, we found that nadroparin did not cause either arrest in G_2/M phase (Fig. 8) or reduction in cyclin B1 and Cdk1 expression (Fig. 9a–d, respectively), suggesting that the mechanisms are different in these different cell types.

Finally, in selected experiments, synthetic pentasaccharide, fondaparinux, was used instead of nadroparin. As shown in Fig. 10, fondaparinux, at 40 IU/ml, caused approximately 8% inhibition in number of viable A549 cells that did not reach statistical significance after three consecutive experiments. Furthermore, as shown in Fig. 10b,c, western blot analysis showed that fondaparinux treatment did not affect cyclin B1 expression.

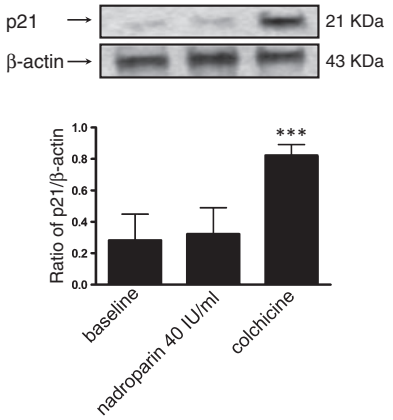

Figure 6. Western blot analysis of the effect of nadroparin on p21 protein levels in A549 cells. Effect of nadroparin on p21 protein levels. Blot is representative of three independent experiments. For densitometric analysis, the resulting bands were quantified using IMAGEJ; data are mean ± SEM from all three experiments. ***$P < 0.0001$ for nadroparin (40 IU/ml) and colchicine-treated versus -untreated cells (ANOVA).

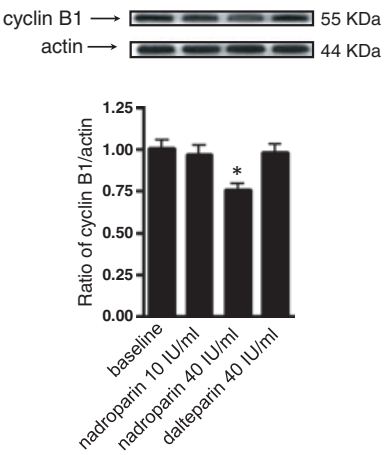

Figure 7. Effect of dalteparin versus nadroparin on cyclin B1 protein levels. Blot is representative of three independent experiments. For densitometric analysis, resulting bands were quantified using IMAGEJ; data are mean ± SEM from three independent experiments. *$P < 0.05$ for nadroparin (40 IU/ml)-treated versus -untreated cells (Student's *t*-test).

Discussion

The possibility that LMWHs interfere with cancer cell proliferation, along with indirect anti-tumour effects mediated, for example, by antiangiogenic properties of certain of these molecules *in vivo* (25, 26), has been postulated based on clinical reports that indicate survival advantage of cancer patients treated with these agents. Our data indicate that, indeed, nadroparin inhibits A549 lung cancer cell proliferation *in vitro*. Induction of apoptosis was not responsible for the observed anti-proliferative effect,

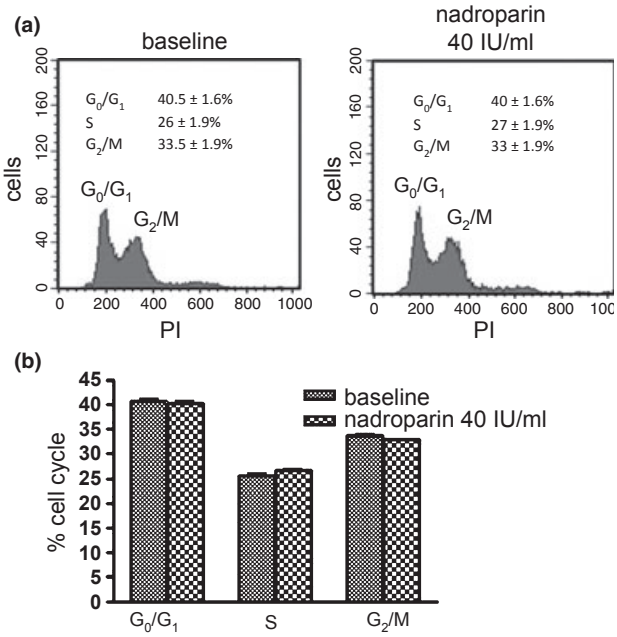

Figure 8. Effect of 48 h nadroparin treatment on CALU-1 cell cycle distribution as assessed by flow cytometric analysis. (a) Histograms from one representative experiment; (b) Mean ± SEM from three independent experiments.

as percentage of $PI^-/A\text{-}V^+$ cells was not affected by treatment. In contrast, we demonstrate an effect on the cell cycle, with arrest in G_2/M phase.

A role for UFH in inhibition of vascular smooth muscle cell proliferation, both *in vitro* and *in vivo*, has long been acknowledged (27,28). Fasciano et al. have extensively investigated the molecular basis of this property of heparin, demonstrating blocking in G_1 to S phase transition mediated by inhibition of Cdk2 activity. Our data, generated with LMWH, nadroparin, as opposed to UFH, and using a lung cancer cell line rather than vascular smooth muscle cells, differ from those of Fasciano, in that in our experimental setting, disruption of the cell cycle takes place at a different level, causing arrest in G_2/M phase.

Progression of cells through the different phases of the cell cycle is controlled by regulated sequential expression and activation of three key classes of regulatory molecules, termed cyclins, Cdk (also referred to as cdc), and Cdki (29–31). In mammalian cells, cyclin B1 forms a complex with Cdk1 defined as the maturation-promoting factor or M phase-promoting factor (MPF) that is essential for the cell's entry into mitosis and progression to complete cell division (32–34). During G_2 phase, cyclin B1/Cdk1 complex, in particularly Cdk1, is inactivated by phosphorylation of two regulatory residues – Thr14/Tyr15. Dephosphorylation of Thr14 and

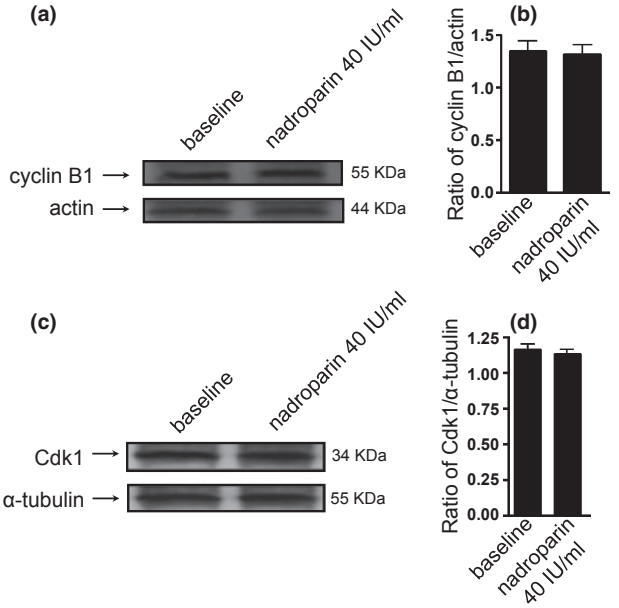

Figure 9. Western blot analysis of the effect of nadroparin on cyclin B1 (a) and Cdk1 (c) in CALU-1 cell line. (a) Effect of nadroparin on cyclin B1 protein levels after treatment with 40 IU/ml nadroparin for 48 h. Blot is representative of three independent experiments; (b) Densitometric analysis of resulting bands. Bands were quantified using IMAGEJ; data are mean ± SEM from three independent experiments. (c) Effect of nadroparin on Cdk1 protein levels after treatment with 40 IU/ml nadroparin for 48 h. Blot is representative of three independent experiments; (d) Densitometric analysis of resulting bands. Bands were quantified using IMAGEJ; data are mean ± SEM from three independent experiments.

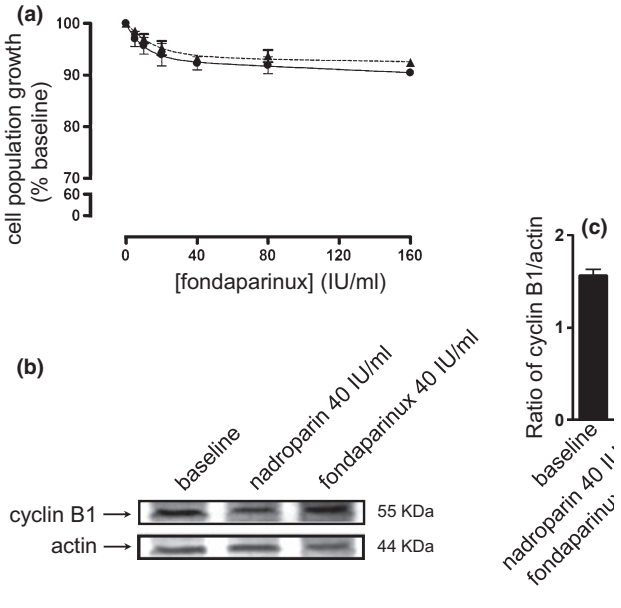

Figure 10. Dose–response effect of fondaparinux on A549 cell population growth (a) determined by MTT assay and western blot analysis on cyclin B1 levels in A549 cell line (b and c). (a) Cells were treated with fondaparinux for 24 h (–▲–) and 48 h (—●—). Data are mean ± SEM of three independent experiments, each performed in quadruplicate. (b) Effect of fondaparinux on cyclin B1 protein levels after treatment with 40 IU/ml fondaparinux for 48 h. Blot is representative of three independent experiments; (c) Densitometric analysis of resulting bands. Bands were quantified using IMAGEJ; data are mean ± SEM from three independent experiments.

Tyr15 by phosphorylating Cdc25C to p-Cdc25C at Ser 216 in late G_2, directly activates cyclin B1/Cdk1 complex and triggers initiation of mitosis (23). As not only Cdc25C but also cyclin B1 has been reported to be necessary for Cdk1 activation, reduced expression of cyclin B1, prior to G_2/M transition, may result in indirect Cdk1 inactivation and the cell cycle will arrest in G_2; thus, the cells cannot enter mitosis.

Our data show reduced synthesis of cyclin B1 protein and decrease in mRNA level when A549 lung cancer cells are incubated with nadroparin; these results are consistent with the hypothesis that this is, at least in part, the mechanism by which this LMWH alters the cell cycle. However, our data indicate that Cdk1 protein expression and its mRNA levels are also impaired by nadroparin. In addition, exposure to nadroparin after 48 h resulted in increase of inactive phosphorylated Cdk1 (Tyr15). Resulting accumulation of Cdk1 in inactive phosphorylated state prevents cells from entering mitosis.

Cdks are initially activated by their association with cyclin subunits and by phosphorylation of threonine plus tyrosine residues. To explain reduction in Cdk1 protein and mRNA expression and increase in p-Cdk1 protein, we hypothesized that nadroparin could affect the Cdc25C pathway and that this might be linked to G_2/M phase arrest. Our data showed that nadroparin downregulated expression of Cdc25C protein and mRNA level; in addition, exposure to nadroparin caused reduction in p-Cdc25C protein expression, an effect potentially responsible for Cdk1 inactivation and for increase in the inactive form of p-Cdk1, after 48 h treatment, that in turn might have contributed to G_2/M phase arrest by preventing phosphorylation of Cdc25C as a late event.

Cdk activity is also negatively regulated by interaction with specific Cdki, which cause a cell cycle block, when overexpressed artificially in several cell lines (35). Two classes of Cdki that negatively regulate cyclin-Cdk-dependent progression of the cell cycle have been defined: INK proteins (p16INK4a, p15INK4b, p18INK4c, and p19INK4d) and Cip/Kip proteins (p21cip1, p27kip1, and p57kip2) (30). p21, also known as Cip1 or WAF1, is a 21 kDa protein initially identified as a cell cycle regulatory protein that can cause cell cycle arrest. Our data indicate that nadroparin did not alter p21 expression, suggesting that the p21 signalling

pathway is not responsible for G_2/M cell cycle arrest in A549 cells.

These alterations in cell cycle kinetics might contribute to better understanding of the cytotoxicity of nadroparin and facilitate its potential use for management of lung cancer.

In the 1980s, development of LMWHs extended and enhanced usefulness of this class of drug, and for many indications, LMWHs have replaced the parent compound, UFH, in therapy and prophylaxis of thromboembolic disorders, due to their higher safety and overall lower cost (36–38). The effect of size and sulphation of various heparin-derived oligosaccharides, on endothelial cell population growth has been investigated. The authors demonstrated that minimum chain length and a certain degree of sulphation are required to control this event. They found that low sulphate oligosaccharides, 18 monosaccharides (the size of fragments obtained by nitrous acid depolymerization of heparin) and larger, were significantly more inhibitory than medium and high sulphate fractions, and whole heparin. Therefore, endothelial cell population growth was highest for the most sulphated oligosaccharides (39).

Of the two LMWHs used in the present work, structural differences between dalteparin and nadroparin result in higher molecular weight profile (6000 Da versus 4300 Da of nadroparin) and a higher sulphate content ($SO3^-/COO^-$ ratio of dalteparin is 2.0/2.5 versus 1.8/2.0 of nadroparin) (40,41). Although dalteparin and nadroparin are both prepared by the same method (16), they do not present identical properties. The different effects of these molecules on regulation of the cell cycle are likely to be dependent on different saccharide size and degree of sulphation. It is therefore important that data obtained with one molecule are not directly extrapolated to another. In keeping with this notion, we observed that nadroparin and dalteparin have different effects on cyclin B1, and confirmed that the latter does not affect its expression, as has previously been reported (13). This, and the observation that nadroparin did not alter cyclin B1 nor Cdk1 expression, and did not cause arrest at G_2/M in CALU-1 cells, suggests that molecular mechanisms by which LMWHs affect lung cancer cell proliferation depend on both the heparin molecule and the cell type.

The synthetic pentasaccharide, fondaparinux, represents the first drug of a new class of anticoagulants that was developed as a highly specific antithrombin (AT)-dependent inhibitor of action of factor Xa (FXa) (42) that has been shown to be a safe and effective alternative to LMWHs in prevention and treatment of venous thromboembolism. Fondaparinux consists of five saccharides comprising the AT-binding sequence of heparin; by binding to AT with very high affinity and specificity, it increases ability of AT to inactivate FXa by a factor of around 300 (43). In contrast to heparin and LMWHs that are a heterogeneous mixture of molecules, fondaparinux is made by chemical synthesis, making it a well-defined drug (42). Using comparable anti-Xa activities, we observed much lower effects of fondaparinux on A549 cell proliferation, and no effect on cyclin B1 expression.

Two recent studies compared effects of fondaparinux with dalteparin and tinzaparin, on human osteoblast and mesenchymal stem cell (MSC) proliferation *in vitro*, respectively. These studies demonstrated that both osteoblast and MSC proliferation were inhibited by addition of LMWHs. In contrast, the pentasaccharide had no effect on osteoblast and MSC proliferation (44,45).

This observation confirms and extends previous data that have shown that anti-proliferative effects of LMWHs in endothelial cells are dependent on molecular weight, and that tetra- penta- and octasaccharides have no anti-proliferative effects (46). Thus, as optimal saccharide sequence for anti-proliferative effects of LMWHs is not identical to the optimal sequence for its anticoagulant effect, potential exists for development of a synthetic oligosaccharide based on nadroparin structure, that retains anti-proliferative effects with minimal or no anticoagulant properties. This molecule might be used at higher concentrations in cancer patients without the risk of bleeding, inherent to comparable doses of LMWHs.

The prognosis of lung cancer remains poor despite advances in our understanding of biology of this disease. LMWHs, already widely used in management of lung cancer patients when required by a high risk of thromboembolic complications, also have the potential to increase life expectancy. Better understanding of the molecular basis of this potential anti-cancer activity of LMWHs will increase our ability to provide optimal use of these drugs. Furthermore, the possibility that a synthetic oligosaccharide chain can be designed to retain anti-proliferative effect of LMWHs minimizing bleeding side effects, might offer a novel therapeutic option to combat this disease.

Conflict of interest

None of the authors have conflicts of interest to disclose.

References

1 Jemal A, Siegel R, Ward E, Hao Y, Xu J, Thun MJ (2009) Cancer statistics, 2009. *CA Cancer J. Clin.* **59**, 225–249.

2 Molina JR, Adjei AA, Jett JR (2006) Advances in chemotherapy of non-small cell lung cancer. *Chest* **130**, 1211–1219.
3 Herbst RS, Heymach JV, Lippman SM (2008) Lung cancer. *N. Engl. J. Med.* **359**, 1367–1380.
4 Kakkar AK, Levine MN, Kadziola Z, Lemoine NR, Low V, Patel HK *et al.* (2004) Low molecular weight heparin, therapy with dalteparin, and survival in advanced cancer: the fragmin advanced malignancy outcome study (FAMOUS). *J. Clin. Oncol.* **22**, 1944–1948.
5 Altinbas M, Coskun HS, Er O, Ozkan M, Eser B, Unal A *et al.* (2004) A randomized clinical trial of combination chemotherapy with and without low-molecular-weight heparin in small cell lung cancer. *J. Thromb. Haemost.* **2**, 1266–1271.
6 Klerk CP, Smorenburg SM, Otten HM, Lensing AW, Prins MH, Piovella F *et al.* (2005) The effect of low molecular weight heparin on survival in patients with advanced malignancy. *J. Clin. Oncol.* **23**, 2130–2135.
7 Conti I, Rollins BJ (2004) CCL2 (monocyte chemoattractant protein-1) and cancer. *Semin. Cancer Biol.* **14**, 149–154.
8 Borsig L, Wong R, Feramisco J, Nadeau DR, Varki NM, Varki A (2001) Heparin and cancer revisited: mechanistic connections involving platelets, P-selectin, carcinoma mucins, and tumor metastasis. *Proc. Natl. Acad. Sci. USA* **98**, 3352–3357.
9 Norrby K, Ostergaard P (1997) A 5.0-kD heparin fraction systemically suppresses VEGF165-mediated angiogenesis. *Int. J. Microcirc. Clin. Exp.* **17**, 314–321.
10 Fasciano S, Patel RC, Handy I, Patel CV (2005) Regulation of vascular smooth muscle proliferation by heparin: inhibition of cyclin-dependent kinase 2 activity by p27(kip1). *J. Biol. Chem.* **280**, 15682–15689.
11 Patel RC, Handy I, Patel CV (2002) Contribution of double-stranded RNA-activated protein kinase toward antiproliferative actions of heparin on vascular smooth muscle cells. *Arterioscler. Thromb. Vasc. Biol.* **22**, 1439–1444.
12 Mousa SA, Petersen LJ (2009) Anti-cancer properties of low-molecular-weight heparin: preclinical evidence. *Thromb. Haemost.* **102**, 258–267.
13 Chen X, Xiao W, Qu X, Zhou S (2008) The effect of dalteparin, a kind of low molecular weight heparin, on lung adenocarcinoma A549 cell line in vitro. *Cancer Invest.* **26**, 718–724.
14 Fareed J, Hoppensteadt D, Schultz C, Ma Q, Kujawski MF, Neville B *et al.* (2004) Biochemical and pharmacologic heterogeneity in low molecular weight heparins. Impact on the therapeutic profile. *Curr. Pharm. Des.* **10**, 983–999.
15 Nicolau JC, Cohen M, Montalescot G (2009) Differences among low-molecular-weight heparins: evidence in patients with acute coronary syndromes. *J. Cardiovasc. Pharmacol.* **53**, 440–445.
16 Linhardt RJ, Gunay NS (1999) Production and chemical processing of low molecular weight heparins. *Semin. Thromb. Hemost.* **25** (Suppl. 3), 5–16.
17 Fareed J, Leong WL, Hoppensteadt DA, Jeske WP, Walenga J, Wahi R *et al.* (2004) Generic low-molecular-weight heparins: some practical considerations. *Semin. Thromb. Hemost.* **30**, 703–713.
18 Laemmli UK (1970) Cleavage of structural proteins during the assembly of the head of bacteriophage T4. *Nature* **227**, 680–685.
19 Barry MA, Behnke CA, Eastman A (1990) Activation of programmed cell death (apoptosis) by cisplatin, other anticancer drugs, toxins and hyperthermia. *Biochem. Pharmacol.* **40**, 2353–2362.
20 Duverger V, Sartorius U, Klein-Bauernschmitt P, Krammer PH, Schlehofer JR (2002) Enhancement of cisplatin-induced apoptosis by infection with adeno-associated virus type 2. *Int. J. Cancer* **97**, 706–712.
21 Ohi R, Gould KL (1999) Regulating the onset of mitosis. *Curr. Opin. Cell Biol.* **11**, 267–273.
22 Lew DJ, Kornbluth S (1996) Regulatory roles of cyclin dependent kinase phosphorylation in cell cycle control. *Curr. Opin. Cell Biol.* **8**, 795–804.
23 Donzelli M, Draetta GF (2003) Regulating mammalian checkpoints through Cdc25 inactivation. *EMBO Rep.* **4**, 671–677.
24 Edelman MJ (2006) Novel cytotoxic agents for non-small cell lung cancer. *J. Thorac. Oncol.* **1**, 752–755.
25 Norrby K (2006) Low-molecular-weight heparins and angiogenesis. *APMIS* **114**, 79–102.
26 Debergh I, Van Damme N, Pattyn P, Peeters M, Ceelen WP (2010) The low-molecular-weight heparin, nadroparin, inhibits tumour angiogenesis in a rodent dorsal skinfold chamber model. *Br. J. Cancer* **102**, 837–843.
27 Castellot JJJ, Addonizio ML, Rosenberg R, Karnovsky MJ (1981) Cultured endothelial cells produce a heparinlike inhibitor of smooth muscle cell growth. *J. Cell Biol.* **90**, 372–379.
28 Clowes AW, Clowes MM (1987) Regulation of smooth muscle proliferation by heparin in vitro and in vivo. *Int. Angiol.* **6**, 45–51.
29 King RW, Jackson PK, Kirschner MW (1994) Mitosis in transition. *Cell* **79**, 563–571.
30 Morgan DO (1995) Principles of CDK regulation. *Nature* **374**, 131–134.
31 Satyanarayana A, Kaldis P (2009) Mammalian cell-cycle regulation: several Cdks, numerous cyclins and diverse compensatory mechanisms. *Oncogene* **28**, 2925–2939.
32 Hartwell LH, Weinert TA (1989) Checkpoints: controls that ensure the order of cell cycle events. *Science* **246**, 629–634.
33 Porter LA, Donoghue DJ (2003) Cyclin B1 and CDK1: nuclear localization and upstream regulators. *Prog. Cell Cycle Res.* **5**, 335–347.
34 Gavet O, Pines J (2010) Progressive activation of cyclin B1-Cdk1 coordinates entry to mitosis. *Dev. Cell* **18**, 533–543.
35 Tanner FC, Yang ZY, Duckers E, Gordon D, Nabel GJ, Nabel EG (1998) Expression of cyclin-dependent kinase inhibitors in vascular disease. *Circ. Res.* **82**, 396–403.
36 Sprague S, Cook DJ, Anderson D, O'Brien BJ (2003) A systematic review of economic analyses of low-molecular-weight heparin for the treatment of venous thromboembolism. *Thromb. Res.* **112**, 193–201.
37 Camporese G, Bernardi E (2009) Low-molecular-weight heparin for thromboprophylaxis. *Curr. Opin. Pulm. Med.* **15**, 443–454.
38 Kakkar VV, Boeckl O, Boneu B, Bordenave L, Brehm OA, Brucke P *et al.* (1997) Efficacy and safety of a low-molecular-weight heparin and standard unfractionated heparin for prophylaxis of postoperative venous thromboembolism: European multicenter trial. *World J. Surg.* **21**, 2–8; discussion 8–9.
39 Sudhalter J, Folkman J, Svahn CM, Bergendal K, D'Amore PA (1989) Importance of size, sulfation, and anticoagulant activity in the potentiation of acidic fibroblast growth factor by heparin. *J. Biol. Chem.* **264**, 6892–6897.
40 Bianchini P, Liverani L, Spelta F, Mascellani G, Parma B (2007) Variability of heparins and heterogeneity of low molecular weight heparins. *Semin. Thromb. Hemost.* **33**, 496–502.
41 Collignon F, Frydman A, Caplain H, Ozoux ML, Le Roux Y, Bouthier J *et al.* (1995) Comparison of the pharmacokinetic profiles of three low molecular mass heparins–dalteparin, enoxaparin and nadroparin–administered subcutaneously in healthy volunteers (doses for prevention of thromboembolism). *Thromb. Haemost.* **73**, 630–640.

42 Turpie AG, Eriksson BI, Lassen MR, Bauer KA (2003) Fondaparinux, the first selective factor Xa inhibitor. *Curr. Opin. Hematol.* **10**, 327–332.
43 Walenga JM, Jeske WP, Bara L, Samama MM, Fareed J (1997) Biochemical and pharmacologic rationale for the development of a synthetic heparin pentasaccharide. *Thromb. Res.* **86**, 1–36.
44 Papathanasopoulos A, Kouroupis D, Henshaw K, McGonagle D, Jones EA, Giannoudis PV (2011) Effects of antithrombotic drugs fondaparinux and tinzaparin on in vitro proliferation and osteogenic and chondrogenic differentiation of bone-derived mesenchymal stem cells. *J. Orthop. Res.* **29**, 1327–1335.
45 Handschin AE, Trentz OA, Hoerstrup SP, Kock HJ, Wanner GA, Trentz O (2005) Effect of low molecular weight heparin (dalteparin) and fondaparinux (Arixtra) on human osteoblasts in vitro. *Br. J. Surg.* **92**, 177–183.
46 Khorana AA, Sahni A, Altland OD, Francis CW (2003) Heparin inhibition of endothelial cell proliferation and organization is dependent on molecular weight. *Arterioscler. Thromb. Vasc. Biol.* **23**, 2110–2115.